Topological-distance-dependent transition in flocks with binary interactions

Biplab Bhattacherjee, Shradha Mishra, and S. S. Manna*
Satyendra Nath Bose National Centre for Basic Sciences, Block-JD, Sector-III, Salt Lake, Kolkata-700098, India
(Received 27 August 2015; published 21 December 2015)

We have studied a flocking model with binary interactions (binary flock), where the velocity of an agent depends on the velocity of only another agent and its own velocity, topped by the angular noise. The other agent is selected as the nth topological neighbor; the specific value of n being a fixed parameter of the problem. On the basis of extensive numerical simulation results, we argue that for $n = 1$, the phase transition from the ordered to the disordered phase of the flock is a special kind of discontinuous transition. Here, the order parameter does not flip-flop between multiple metastable states. It continues its initial disordered state for a period t_c, then switches over to the ordered state and remains in this state ever after. For $n = 2$, it is the usual discontinuous transition between two metastable states. Beyond this range, the continuous transitions are observed for $n \geqslant 3$. Such a system of binary flocks has been further studied using the hydrodynamic equations of motion. Linear stability analysis of the homogeneous polarized state shows that such a state is unstable close to the critical point and above some critical speed, which increases as we increase n. The critical noise strengths, which depend on the average correlation between a pair of topological neighbors, are estimated for five different values of n, which match well with their simulated values.

DOI: 10.1103/PhysRevE.92.062134 PACS number(s): 64.60.Cn, 64.60.De, 89.75.Fb, 05.45.−a

I. INTRODUCTION

The phenomenon of collective behavior (CB) is being studied with great interest in systems exhibiting nonequilibrium phase transition under driven noise [1–7]. When the noise parameter is tuned to a vanishingly small value, such a system, while evolving dynamically from any arbitrary initial state, spontaneously arrives at an ordered state. On the other hand, for stronger noise the order parameter vanishes [8]. In some models studied in the literature, the nature of the associated transition has been suggested to be "continuous" [8–12], whereas in some other examples "discontinuous" transitions have been claimed [13,14]. The dynamical behavior of an agent is determined by its interaction with other agents in its local neighborhood, where the neighborhood is determined in terms of Euclidean distance [8] or topological distance [9,10,15,16].

In this paper, we have studied the dynamics of binary flocks with angular noise, where an agent interacts only with its nth topological neighbor. Our extensive numerical study indicates that for $n = 1$ and 2, the order-to-disorder transition is discontinuous, but it is continuous for $n \geqslant 3$.

The essential idea of CB stems in the common behavior of a collection of agents. Expectedly, a flock of birds is a typical example of such a collection [17]. In such a collection, agents are generally considered as short-sighted. To elaborate, an individual agent interacts with a group of other agents within a small neighborhood around it, who in turn interact with their neighbors and so on. Thus, information propagates between a pair of agents, even though they are positioned at a large distance of separation from each other and are able to influence each other. Eventually, all agents in the entire flock become correlated, and the whole group acts in unison. Therefore, even a short-range interaction among the agents results in a unique global behavior of the entire group. Such a flock pattern is called "cohesive" when, on the average, each agent maintains a certain characteristic distance from other agents. At the same time they are said to be "coherent," since all agents travel along the same direction in space. This type of motion indicates that a long-range correlation has set in among the agents. The question is, what kind of models or local interactions ensure such global correlations?

The Vicsek model is a simple and well-known model in CB [8]. In its two-dimensional version, agents are released at random locations with randomly assigned velocities within a unit square box, fitted with periodic boundary condition. At any arbitrary intermediate time during the dynamical evolution, the direction of velocity of each agent i is oriented along the resultant velocity $\mathbf{v}_i(R)$ of all agents within a range R around i. The speed of each agent is assumed to be the same and is equal to a constant v. However, in practice each agent may make an error in judging the resultant direction of motion and therefore a noise is introduced by topping the orientation angle of $\mathbf{v}_i(R)$ by a random amount $\Delta\theta$ selected with uniform probability. Every agent is then displaced along the updated velocity direction. This update takes place synchronously, i.e., velocities of all agents at time $(t + 1)$ are determined using the velocities of all agents at time t. A coherent phase is observed in the noise-free case with high agent densities. Moreover, a continuous phase transition is observed on increasing the strength of noise as the mean flock speed continuously decreases to zero. Moreover, facets like high density traveling bands occurring at low noise were revealed in later studies [13,18] and arguments were put forward in favor of a discontinuous transition. Further, it has been argued that by tuning the magnitude of the velocity of agents one can switch over from continuous to discontinuous transitions [19].

On the other hand, a number of studies have been done where the interacting neighborhood is determined using the topological distance. For example, in Ref. [15], an agent interacts only with its Voronoi neighbors. Therefore, even

*manna@bose.res.in

when the agent density is low, and the typical distance between the agents is quite large, an agent interacts with its topological neighbors. It was observed that the behavior of such a flock is somewhat different from the one defined in terms of metric distance [15]. Also, the metric free topology was used in the hydrodynamic description of self-propelled agents where the neighbors are determined by topological distance instead of the metric distance [16]. Among other results, it was claimed that the deterministic continuous theories of metric-free flock are formally equivalent to their metric counter parts.

We describe our flocking model with binary interactions in Sec. II. Subsequently, the simulation results for five different cases, namely from $n = 1$ to 5, are described in Sec. III. In Sec. IV we have discussed the phenomenon of persistence as well as the information spreading processes associated in this model. Section V describes the theoretical analysis using hydrodynamic equations of motion for our binary flock. We summarize in Sec. VI.

II. MODEL

In our binary flock, the direction of velocity of any arbitrary agent i depends on the direction of velocity of its nth nearest neighbor j and its own velocity. Let us assume that with respect to any arbitrary reference direction, the velocity directions in time t of the ith and jth agents are $\theta_i(t)$ and $\theta_j(t)$, respectively. Then, in the next time step $t + 1$, the updated velocity direction will be

$$\theta_i(t+1) = \tan^{-1}\left[\frac{\sin(\theta_i(t)) + \sin(\theta_j(t))}{\cos(\theta_i(t)) + \cos(\theta_j(t))}\right] + \Delta\theta, \qquad (1)$$

where $\Delta\theta$ is a random top-up angle, that represents the noise variable. Its value is drawn freshly from the uniform distribution within the range $\{-\eta/2, \eta/2\}$, η being the continuously tunable strength of the noise parameter. The agents' velocities are updated synchronously. Therefore, the entire set of the velocity angles $\theta_i(t + 1)$ are determined simultaneously using the complete set of $\theta_i(t)$ for all i. The order parameter is determined by the magnitude of the resultant velocity vector, scaled by the speed v and averaged over all N agents,

$$V(t) = \frac{1}{Nv}|\Sigma_i \mathbf{v}_i(t)|. \qquad (2)$$

In the following, we have considered five different cases for five different values of n, namely 1 to 5. Within our numerical accuracy we present evidences to claim that the system undergoes an order-to-disorder phase transition with respect to the noise parameter η, the system has discontinuous transitions for $n = 1$ and 2; where as for $n \geqslant 3$ the nature of transition is continuous.

Numerical simulations have been performed on a $L \times L$ planer area. The density and the speed of agents are kept fixed at $\rho_0 = 1/8$ agents per unit area and $v = 1/2$ in all calculations. In all simulations we have kept the density constant but varied the system size L.

III. THE RESULTS

A. The $n = 1$ case

For $n = 1$, every agent's velocity is determined by its own velocity and that of its first nearest neighbor. In general, if the jth agent is the first nearest neighbor of the ith agent, that does not necessarily imply that i is also the first nearest neighbor of j. However, with a small probability this may actually happen, when both the ith and the jth agents are mutually dependent on each other for a while. Typically this happens when they are spatially close to each other but at the same time far away from all other agents. In this situation they would form a very strongly bound pair. For example, for $\eta = 0$, both of them are completely synchronized and move along the same direction in parallel straight lines with exactly the same velocity, until they come in the close proximity to a third agent so that i and j cease to be mutually nearest neighbors any longer. On the other hand, for small values of $\eta > 0$, though their motion is random, yet they perform a nearly synchronized motion.

We start exhibiting the variation of the order parameter $V(t,\eta,L)$ against time at different noise levels η in Fig. 1. The time evolution of the system starts from the same initial configuration of the agents at time $t = 0$, that is, the same spatial locations as well as their random velocities, are used for all values of η. For small values of η, the system is in the ordered phase with relatively large value of the $V(t,\eta,L)$ that fluctuates around a steady mean value in the stationary state. On the other hand, as η is gradually increased, the system moves into the disordered phase, the mean value $\langle V(t,\eta,L)\rangle$ of the order parameter gradually decreases. The order-to-disorder transition takes place in between these two regimes. It has been

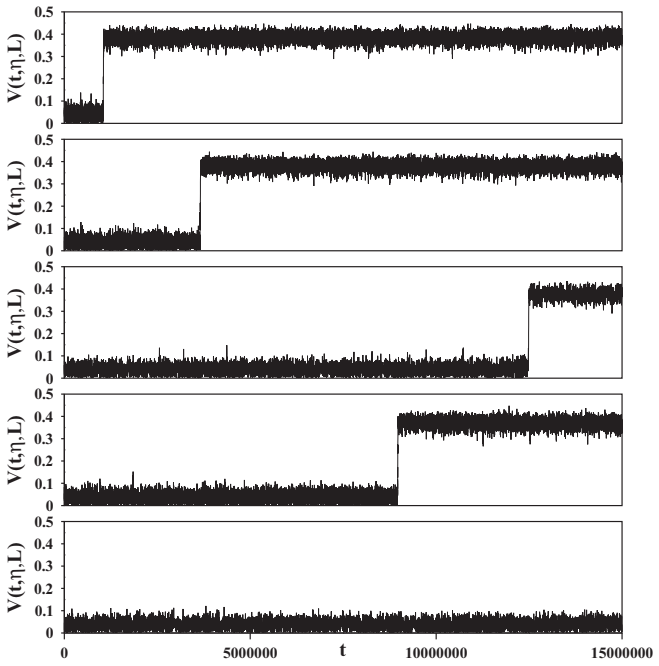

FIG. 1. For $n = 1$, L =512, and $\rho_0 = 1/8$. Plot of the order parameter $V(t,\eta,L)$ against time t. The switching times and their corresponding noise strengths are t_c = 1 047 100 ($\eta = 0.1184$), 3 650 100 (0.1188), 12 484 400 (0.1190), and 8 964 900 (0.1196) and for $\eta = 0.1200$ the system never switched over to the ordered state.

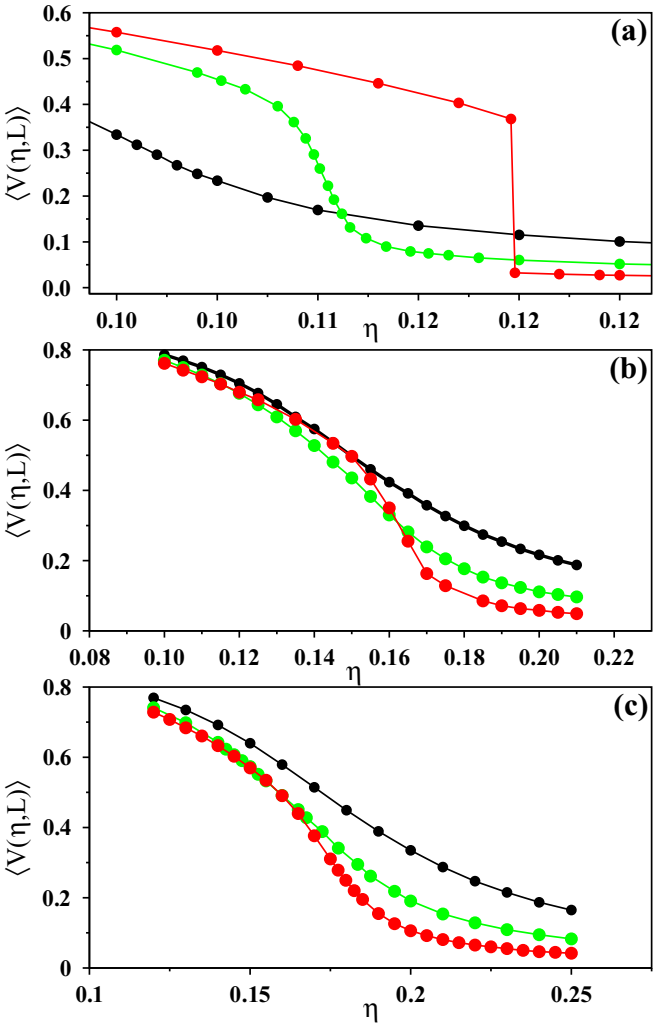

FIG. 2. (Color online) Plot of the order parameter $\langle V(\eta,L)\rangle$ with $\rho_0 = 1/8$ against noise parameter η for the system size $L = 128$ (black), 256 (green), and 512 (red) for (a) $n = 1$, (b) $n = 4$, and (c) $n = 5$.

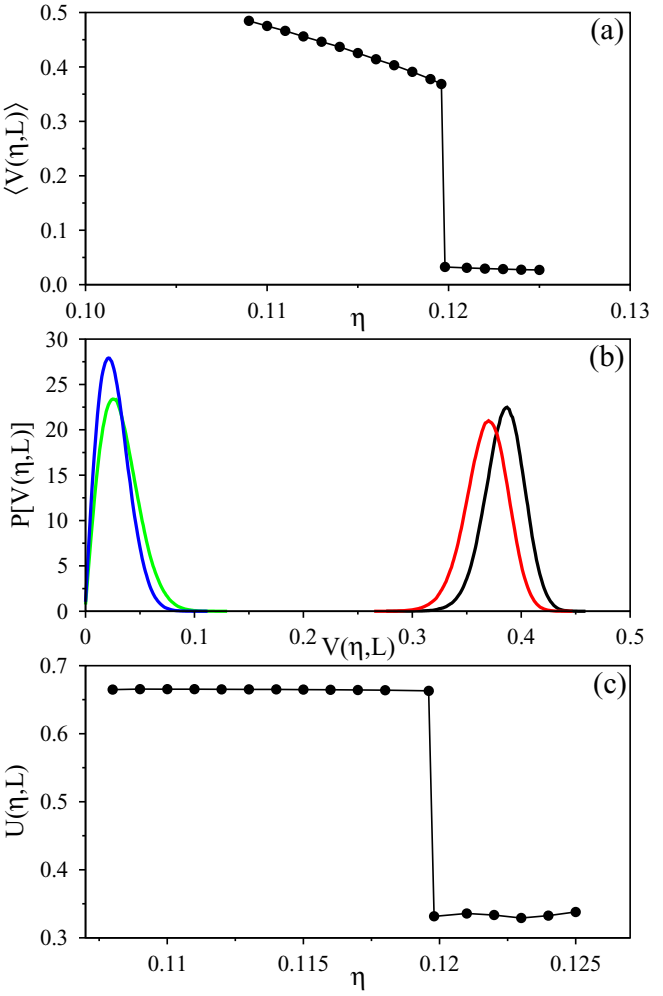

FIG. 3. (Color online) For $n = 1$, $L = 512$, and $\rho_0 = 1/8$. (a) Plot of the order parameter $\langle V(\eta,L)\rangle$ against noise parameter η exhibits a discontinuous jump at $\eta = 0.1197$. (b) The probability density of the order parameter $P[V(\eta,L)]$ plotted against $V(\eta,L)$; for the ordered state: $\eta = 0.1184$ (black) and 0.1196 (red) and for the disordered state $\eta = 0.1198$ (green) and 0.1250 (blue) in the sequence from right to left. (c) Binder cumulant $U(\eta,L)$ plotted against η jumps discontinuously from ≈0.663 to ≈0.332 at $\eta_c = 0.1197$.

observed that typically the system starts in a disordered state but after some time, say t_c, it switches over to the ordered state when η is comparatively small. It is also noticed that the switching time becomes increasingly larger as η is gradually tuned to larger values.

In usual discontinuous transition and close to the critical point, the system is found to be in multiple metastable states. Therefore, while in the stationary state, the system often switches back and forth between different metastable states [20]. In our system, this scenario has been observed for small system sizes, e.g., $L = 128$ and 256 but not for $L = 512$. In Fig. 2(a) we have displayed the finite-size effect on the variation of the order parameter against noise strength η for the same three system sizes. Though the variation is continuous for the two smaller lattice sizes, it is apparent that with increasing the system size, the variation becomes increasingly sharper at the transition point. However, for the largest system size of $L = 512$, the variation of the order parameter has been observed to be clearly discontinuous. In contrast to the ususal scenario, our large time (up to 55 million steps) simulation indicates that here the system picks up one of the two possible states, i.e., either the ordered state or the disordered state and remains in that state ever after. Therefore, the averaged value of the order parameter $\langle V(\eta,L)\rangle$ has been measured after the switching time t_c. Consequently, a plot of $\langle V(\eta,L)\rangle$ against η in Fig. 3(a) exhibits a clear discontinuous jump at the value of $\eta_c = 0.1197(1)$, exhibiting that it is indeed a discontinuous transition. Individual error bar of every point has been calculated and they have been found to be very small, of the order of the size of the symbols used for the plots.

The probability distribution of the order parameter $P[V(\eta,L)]$ against $V(\eta,L)$ has been studied next [Fig. 3(b)]. The distribution is observed to be a singly peaked curve. The position of the peak is large for the ordered state and small for the disordered state. The probability distribution abruptly shifts to the small values of V as the noise parameter η is gradually increased. In two such plots for $\eta = 0.1184$ and

0.1196 the system is in the ordered state. However, when η is increased by the smallest amount of 0.0002 to the value 0.1198, the system makes a transition to the disordered state and the distribution discontinuously shifts a large amount to the small regime of V.

The fourth-order Binder cumulant $U(\eta,L)$ is defined as

$$U(\eta,L) = 1 - \frac{\langle V^4(\eta,L)\rangle}{3\langle V^2(\eta,L)\rangle}. \quad (3)$$

Figure 3(c) shows the variation of $U(\eta,L)$ against η. It is very much consistent with the limiting values, that is, $U(\eta,L) \approx 2/3$ for $\eta < \eta_c$ and $U(\eta,L) \approx 1/3$ for $\eta > \eta_c$. The specific value of η where the jump in U takes place is $\eta_c = 0.1197$ and this is recognized as the critical value η_c of the noise parameter.

B. The $n = 2$ case

Here, the velocity of an agent i is determined by the velocity of its second nearest neighbor j and its own velocity. Therefore, the presence of a third agent, say the kth agent, is necessary. For both ith and jth agents, the kth agent may act as their first neighbor. In turn, for the kth agent, the jth agent may be the first neighbor and the ith neighbor may be the second neighbor. This is one special combination in which all three agents mutually depend on one another and form a stable cluster. However, at every time step the noise feeds in fresh randomness. When a fourth agent comes close to this cluster, the cluster may not be stable any longer.

It is first observed that unlike the $n = 1$ case, very close to the critical point η_c, the order parameter $V(t,\eta,L)$ fluctuates between its values in the ordered and the disordered states (Fig. 4). The time averaged value of the order parameter $\langle V(\eta,L)\rangle$ in the stationary state varies continuously with the noise parameter η as shown in Fig. 5(a). It assumes high values for small η and gradually decreases as η increases. Around $\eta_c = 0.140$, its value decreases continuously at the fastest rate. For $\eta > \eta_c, \langle V(\eta,L)\rangle$ gradually vanishes. This is also demonstrated in Fig. 5(b) where the probability density of $V(\eta,L)$ has been plotted for five different values of η, namely, 0.138, 0.139, 0.140, 0.141, and 0.142. While for $\eta = 0.138$ and 0.142, the distributions have single maximum, for the intermediate values double maxima appears. For example, for $\eta = 0.139$ the height of the right peak is larger than that of the left peak, for $\eta = 0.140$ both peaks are of nearly same heights whereas for $\eta = 0.141$ the left peak is taller than the right peak. This implies that while $\eta = 0.139$ and 0.141 are in the subcritical and supercritical regimes, respectively, $\eta = 0.140$ is nearly the value of the critical noise.

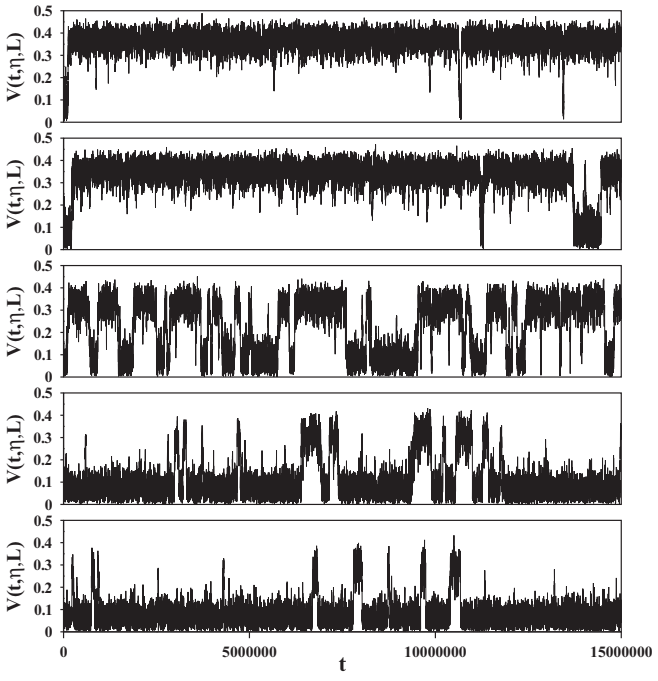

FIG. 4. For $n = 2$, $L = 512$, and $\rho_0 = 1/8$, order parameter $V(t,\eta,L)$ against time t for $\eta = 0.138, 0.139, 0.140, 0.141$, and 0.142 exhibited from top to bottom. The top and bottom ones are almost completely in the ordered and the disordered phases, respectively. Three intermediate plots show existence of metastable stationary states.

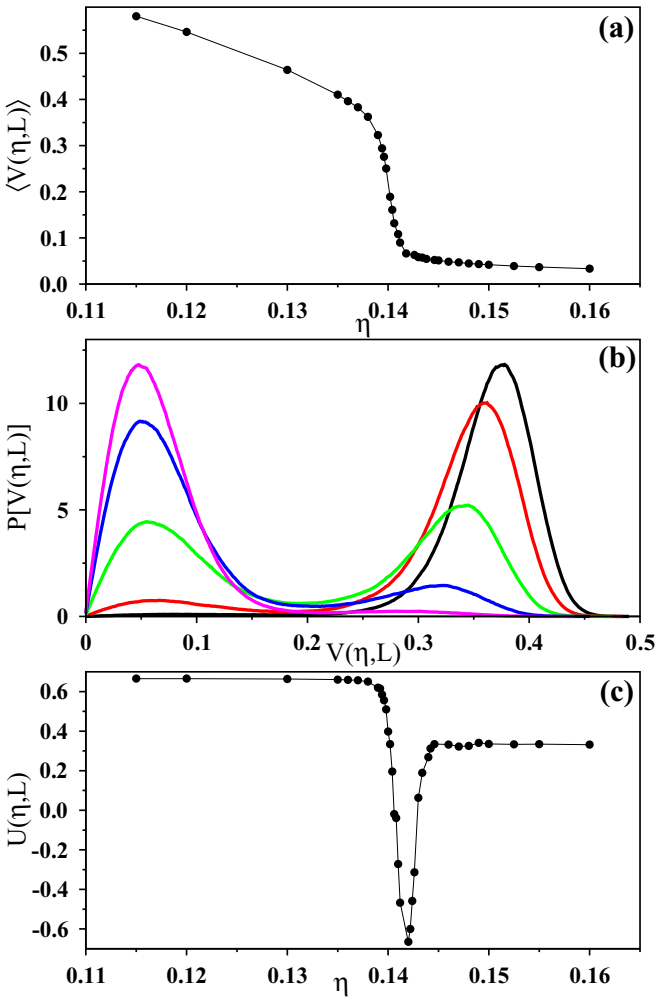

FIG. 5. (Color online) For $n = 2$, $L = 512$, and $\rho_0 = 1/8$. (a) The average value of the order parameter $\langle V(\eta,L)\rangle$ plotted against the noise parameter η. The plot exhibits a sharp, yet continuous variation at $\eta = 0.1400$. (b) The probability density of the order parameter $P[V(\eta,L)]$ for $\eta = 0.1380$ (black), 0.1390 (red), 0.1400 (green), 0.1410 (blue), and 0.1420 (magenta), in the sequence from right to left. (c) Binder cumulant $U(\eta,L)$ plotted against η. At $\eta_c = 0.1400$ its value drops from $\approx$0.66 to ≈ -0.7.

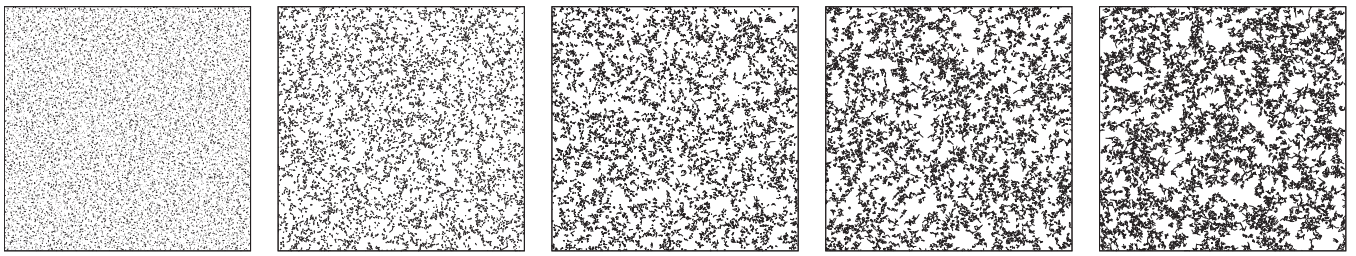

FIG. 6. The spatial network of interaction links for $L = 512$, $\rho_0 = 1/8$, and $\eta = \eta_c(L)$. Every agent is connected to its nth neighbor. Snapshots have been shown for $n = 1$ to 5 (from left to right).

The Binder cumulant $U(\eta,L)$ has been displayed in Fig. 5(c). Because of the existence of the multiple metastable states, a sharp dip in the Binder cumulant exists. This is the typical signature of a discontinuous transition as observed previously in the metric distance dependent Vicsek model [8] occurring at $\eta \approx 0.140$ for $n = 2$.

To see the spatial structure of the flock one can construct the contact network. It is straightforward to define an Euclidean directed network with the binary flock. Here the agents are the nodes, and a directed link is introduced from agent i to agent j if j is the topological neighbor of i. In Fig. 6 the stationary state spatial patterns of such networks have been shown for the critical noise η_c and for $n = 1$ to 5, and for $L = 512$ and $\rho_0 = 1/8$. The spatial distribution of agents are most uniform for $n = 1$. Then as the value of n increases, the agent distribution become more and more heterogeneous.

C. The $n \geqslant 3$ cases

The situation is completely different in the $n \geqslant 3$ cases when we consider the variation of the order parameter $V(t,\eta,L)$ against time t. Neither we see any switching over from the disordered to the ordered state as in $n = 1$ case, nor we observed incessant flip flop between the metastable states of the ordered and disordered states as in $n = 2$ case. The effect on the order parameter due to the finite size of the system have been shown in Figs. 2(b) and 2(c) for $n = 4$ and $n = 5$, respectively. Again its variation becomes increasingly sharper as the system size increases, but remain continuous within the entire range, typical of continuous transition. It is also observed, for $n = 3$, 4, and 5, that the width of fluctuation of $V(t,\eta,L)$ becomes increasingly larger as the critical noise strength $\eta_c(L)$ is approached continuously either from the ordered or from the disordered side. At $\eta = \eta_c(L)$, the fluctuation is maximum (not shown). Very similar are the situation for the cases of $n = 4$ and 5. No discontinuous change in the average value of the order parameter has been detected. In Fig. 7(a) we exhibit the variation of $\langle V(\eta,L)\rangle$ against η for $n = 3$, 4, and 5. Its variation near the critical point is the sharpest for $n = 3$, less sharp for $n = 4$, and most flat for $n = 5$. The critical noise strengths η_c has been estimated to be 0.151, 0.162, and 0.180, respectively, for $L = 512$.

In Fig. 7(b), the probability distribution of the order parameter are shown again for $n = 3, 4$, and 5. Each curve has a single maximum and the peak continuously shifts from high to low value with increasing noise strength. In the ordered state, because of nonzero value of the order parameter, the locations of the three curves are at the right side of Fig. 7(b). Similarly the three peaks at the left side correspond to strong noise so that order parameters are nearly zero. Thus, the transition

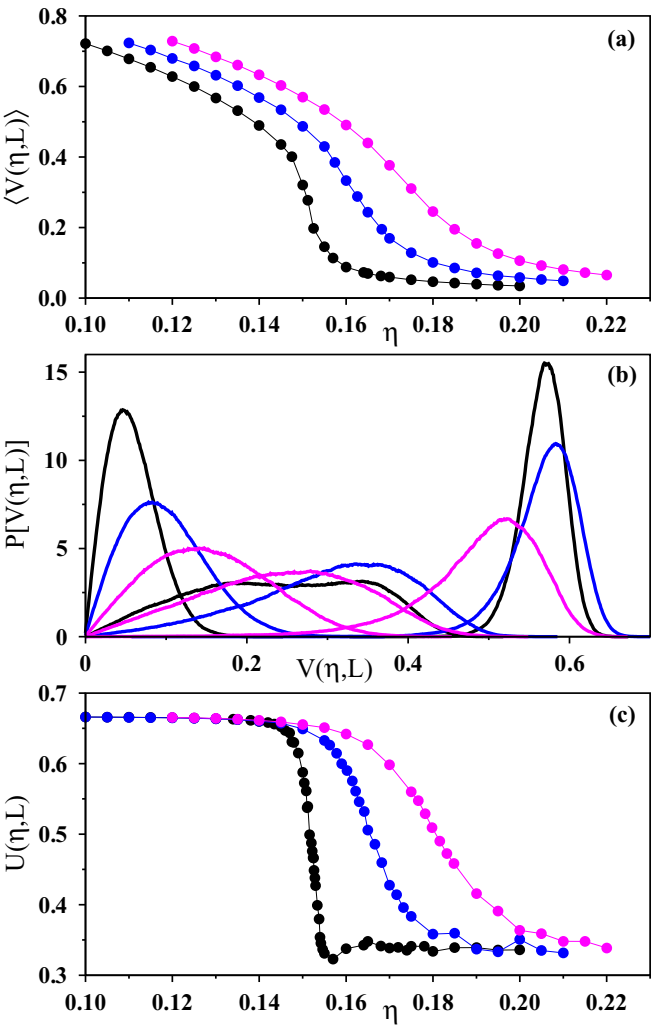

FIG. 7. (Color online) For $L = 512$, $\rho_0 = 1/8$ data for $n = 3$ (black), $n = 4$ (blue), and $n = 5$ (magenta) are shown. (a) The order parameter $\langle V(\eta,L)\rangle$ plotted against η, the plots exhibit sharp but continuous decrease around the critical noise strength $\eta_c(L)$. (b) The probability density of the order parameter $P[V(\eta,L)]$ has been plotted against $V(\eta,L)$. The three peaks on the right correspond to the noise levels of the ordered state, three peaks on the left correspond to the disordered phase, whereas the three curves at the intermediate region have been simulated with $\eta \approx \eta_c(L)$. (c) On increasing η, the Binder cumulant $U(\eta,L)$ decreases continuously from ≈0.66 and attains its disordered phase value ≈0.33 for $\eta > \eta_c(L)$.

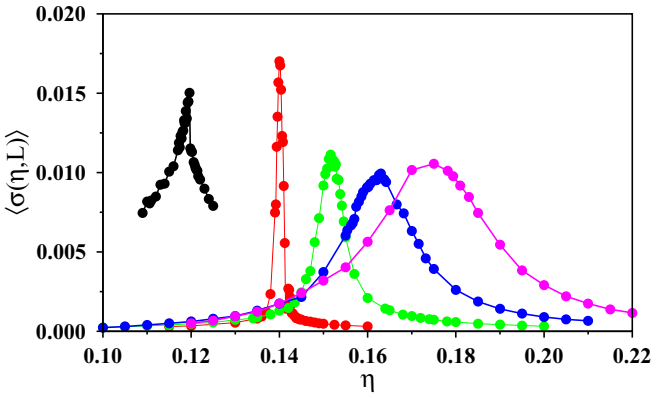

FIG. 8. (Color online) For $L = 512$, $\rho_0 = 1/8$ the standard deviation $\sigma(\eta,L)$ of the order parameter has been plotted against η for $n = 1$ (black), $n = 2$ (red), $n = 3$ (green), $n = 4$ (blue), and $n = 5$ (magenta).

from ordered state to a disordered state exhibits the typical signatures of continuous transition.

The fourth-order Binder cumulants $U(\eta,L)$ have been exhibited in Fig. 7(c). They show a continuous transition from its ordered phase value 2/3 to its disordered phase value 1/3 without any sharp discontinuous jump or any dip to a negative value at any intermediate noise strength η. The decrease was most sharp for $n = 3$, less sharp for $n = 4$, and even less sharper for $n = 5$.

The standard deviation $\sigma(\eta,L)$ of the order parameter has also been studied for different values of n and its variation has been observed against η in Fig. 8. Each curve has a maximum at the critical noise value η_c and $\sigma(\eta,L)$ decays on both sides of η_c.

IV. STUDYING DIFFERENT CHARACTERISTIC TIMES

A. Persistence times

In this section, we study the persistence time distribution for the agents. Persistence time τ for an agent i is a certain interval of time through which any other agent interacts with i. At each time instant, every agent i has another agent j to interact. The interaction partner of i changes from one agent to another agent, and then to another agent, etc., and therefore the agent i passes through a series of persistence times $\tau_1,\tau_2,\tau_3,...$, etc. In the stationary state, we have collected data of these persistence times for each individual agent and have drawn the probability distribution $P(\tau,\eta)$. We have observed that for a fixed density ρ_0 of agents, this distribution does not depend significantly on the system size L, in contrast it does depend very strongly on the noise parameter η. It is apparent, intuitively, that as η decreases there is less fluctuation in the paths of the agents and therefore the typical persistence time gets longer. Consequently, the persistence time distribution gets elongated over a larger period.

In Fig. 9(a) we have shown the plots of persistence time distributions $P(\tau,\eta)$ against τ. On the other hand, three plots for three different values of the noise parameter η differ quite a lot. On a double logarithmic scale the intermediate region of each curve is quite straight and the extent of this regime gets

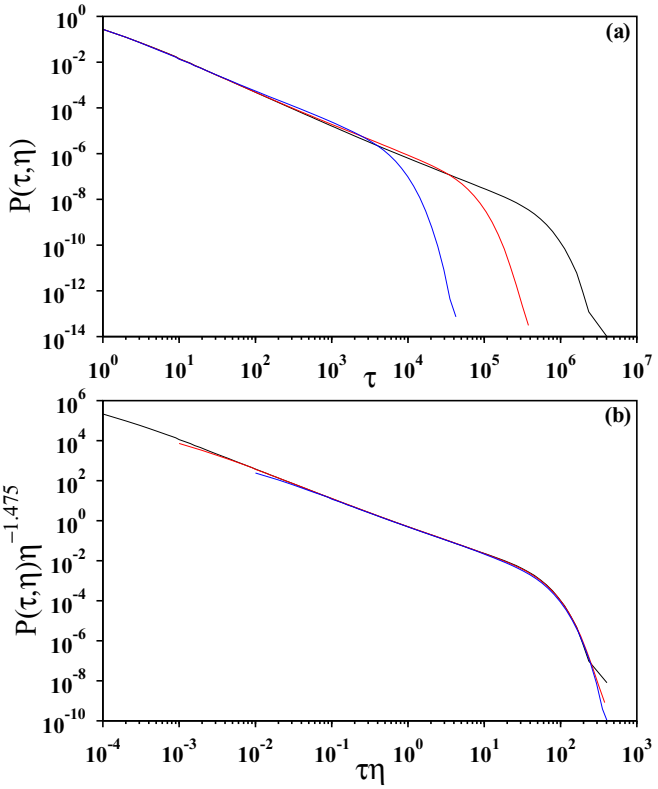

FIG. 9. (Color online) For $n = 1$, $L = 128$, and $\rho_0 = 1/8$. (a) The persistence time distribution $P(\tau,\eta)$ plotted against τ for $\eta = 0.0001$ (black), 0.001 (red), and 0.01 (blue) using log - log scale. (b) The coordinate axes have been rescaled using η^{ζ_1} and $\eta^{-\zeta_2}$ with the best estimates of $\zeta_1 = 1.0$ and $\zeta_2 = 1.475$. This gives the persistence time distribution exponent $\gamma = \zeta_2/\zeta_1 \approx 1.48(2)$.

elongated as $\eta \to 0$. This indicates that the persistence time distribution is likely to follow a simple power law distribution in the limit of $\eta \to 0$,

$$P(\tau) \sim \tau^{-\gamma}, \tag{4}$$

where γ is an exponent, and its value has been estimated by the scaling analysis with respect to η. As η increases the value of the typical persistence time becomes shorter and therefore the extent of the region of validity of the power law also shortens. However, it has been observed that a nice scaling analysis can be performed using this data. In Fig. 9(b) we have replotted the same data after scaling the coordinate axes with η^{ζ_1} and $\eta^{-\zeta_2}$, where $\zeta_1 = 1.0$ and $\zeta_2 = 1.475$. Therefore, the scaling form is

$$P(\tau,\eta)\eta^{-\zeta_2} \sim \mathcal{G}[\tau\eta^{\zeta_1}]. \tag{5}$$

This gives the persistence time distribution exponent $\gamma = \zeta_2/\zeta_1 \approx 1.48(2)$.

B. Information spreading times

During the dynamical evolution of the binary flock, every agent comes in contact with a large number of other agents. Let us assume that at a certain time instant, when the system has settled in its stationary state, a particular agent receives some specific information at time $t = 0$. At time $t = 1$,

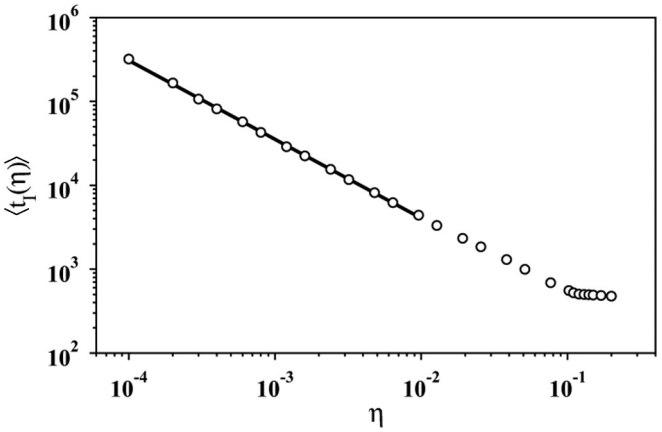

FIG. 10. For $n = 1, L = 256$, and $\rho_0 = 1/8$. The average spreading time $\langle t_I(\eta)\rangle$ has been plotted against η on a double logarithmic scale. The slope of the straight line is the value of the spreading exponent κ defined in Eq. (6) and has the value ≈0.94.

this information is shared with its topological neighbor with probability one. Generally, at any arbitrary intermediate time, all agents having this piece of information share it with their topological neighbors, and this procedure continues. Therefore, after a certain time $t_I(\eta,L)$, the entire collection of agents will be having this information. We call this time the information spreading time t_I, and would like to study how its averaged value $\langle t_I(\eta,L)\rangle$ depends on the noise strength η. It is intuitively clear that the smaller the strength of the noise, the longer is the contact time between the two agents. Therefore, we expect that as $\eta \to 0$, the average contact time would gradually increase. In fact, in the limiting situation of $\eta \to 0$, all agents will be completely coherent in the stationary state. In this situation if there are more that one cluster, these clusters would maintain the separate identities and would never merge. In this case the spreading time is infinity, otherwise it is finite. When $\eta > 0$, the spreading time decreases on the average and we find that it decreases as a power law.

In Fig. 10 we exhibit the estimates of $\langle t_I(\eta,L)\rangle$ against η on a double logarithmic case. The plot appears to fit a nice straight line, and the linearity ends at $\eta = \eta_c$ where it becomes horizontal. Beyond η_c the flock is randomized, the order parameter has the vanishingly small value. Therefore, the average spreading time remains the same, and the curve becomes horizontal.

Therefore, within the range $\eta < \eta_c$, the average spreading time follows a power law decay,

$$\langle t_I(\eta,L)\rangle \sim \eta^{-\kappa}, \tag{6}$$

where $\kappa \approx 0.94(2)$ has been estimated.

V. THEORETICAL ANALYSIS

A. Hydrodynamic equations of motion for binary flocks

We can also estimate the critical noise strengths as we increase the topological neighbor number n to higher values, using the coarse-grained hydrodynamic equations of motion derived from microscopic rule for particle moving along its heading direction with speed v and orientation update for binary flocks as defined in Eq. (1). In our topology-dependent binary interaction model critical point depends on the strength of interaction between the two binary pairs. Strength of interaction can be calculated using angular correlation of two interacting agents. We find the dependence of critical noise strength on interacting binary angular correlation $\alpha(n) = \langle \mathbf{m}_i \mathbf{m}_{\rm in}\rangle$, where $\mathbf{m}_i = (\cos(\theta_i), \sin(\theta_i))$ and $\mathbf{m}_{\rm in}$ is the direction of ith and its nth interacting agent, $\langle ...\rangle$ is average over all possible interacting pairs in the system. We feed the value of $\alpha(n)$ for $n = 1$ to 5 from the microscopic simulation and estimate the critical noise strengths for different n values and compare them with numerical estimates $\eta_c(n)$.

Using the update rule for the position $\mathbf{R}_i$ and orientation θ_i of the ith agent we can write the coarse-grained hydrodynamic equations of motion for density and polarization order parameter defined as

$$\rho(\mathbf{r},t) = \sum_i \delta[\mathbf{r} - \mathbf{R}_i(t)], \tag{7}$$

$$\mathbf{P}(\mathbf{r},t)\rho(\mathbf{r},t) = \sum_i \mathbf{m}_i \delta[\mathbf{r} - \mathbf{R}_i(t)], \tag{8}$$

coarse-grained equation for density is same as previously derived in Ref. [21] for metric distance model

$$\frac{\partial \rho}{\partial t} = -v\nabla \cdot (\mathbf{P}\rho) + D_\rho \nabla^2 \rho, \tag{9}$$

but order parameter equation will be different with no explicit density dependence of alignment term,

$$\frac{\partial \mathbf{P}\rho}{\partial t} = \alpha_1(\eta,\alpha)\mathbf{P}\rho - \alpha_2(\mathbf{P}\cdot\mathbf{P})\mathbf{P}\rho + -\frac{v_1}{2}\nabla\rho + D_P\nabla^2 P, \tag{10}$$

where $\alpha_1(\eta,\alpha) = [\frac{(1-2\eta^2)2}{\sqrt{2(1+\alpha)}} - 1]$ and v is the self-propelled speed of the particle; D_ρ and D_P are the diffusion constants in density and order parameter equations, and α_2 is in general a function of microscopic parameters of the model, but we treat α_2 as constant. Because of Galilean invariance [2], Eq. (10) in general has convective nonlinearities $\propto \mathbf{P}\nabla\mathbf{P}$, but close to order-disorder transition this effect is negligible, hence it has been ignored. The mean field value of critical noise strength η_c is obtained where the coefficient $\alpha_1(\eta,\alpha)$ vanishes,

$$\eta_c = \frac{1}{\sqrt{2}}\left[1 - \frac{1}{\sqrt{2}}\sqrt{(1+\alpha)}\right]^{1/2}. \tag{11}$$

Critical value of noise at which the transition takes place depends very much on the angle-angle correlation $\alpha(n)$ between the agent and its binary pair. The more they are correlated, the more the value of the critical noise strength $\eta_c(n)$ shifts towards the smaller values. In Fig. 11 we plot and compare the values of $\eta_c(n)$ obtained analytically as well as numerically for $n = 1$ to 5.

B. Linear stability of homogeneous polarized state close to order-disorder transition

Steady state solution of homogeneous Eqs. (9) and (10) are $\rho = \rho_0$ and $\mathbf{P} = P_0\hat{\mathbf{z}}$. We add small perturbations $\rho = \rho_0 + \delta\rho$ and $\mathbf{P} = (P_0 + \delta P_z)\hat{\mathbf{z}} + \delta P_x \hat{\mathbf{x}}$ and we can write the linearized equations of motion for small perturbations, $\delta\rho, \delta P_x$

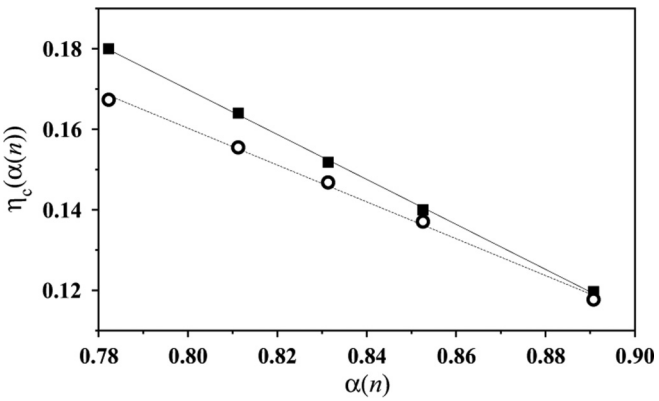

FIG. 11. Plot of mean-field estimate of the critical noise strength $\eta_c(n)$ vs. angle-angle correlation $\alpha(n)$ averaged over all possible interacting pairs. The upper curve (filled squares, solid line) represents the numerical data, whereas, the lower curve (opaque circles, dashed line) represents the analytical result (Eq. (11) in the text).

and δP_z,

$$\partial_t \delta\rho = -vP_0(\partial_z\delta\rho + \partial_x\delta\rho) - v\rho_0(\partial_z\delta P_z + \partial_x\delta P_x) + D_\rho\nabla^2\delta\rho, \tag{12}$$

$$\partial_t \delta P_z = 2P_0^2\alpha(\eta)\delta P_z - \frac{v}{2\rho_0}\delta_z\delta\rho + D_P\nabla^2\delta P_z, \tag{13}$$

$$\partial_t \delta P_x = -\frac{v}{2\rho_0}\delta_x\delta\rho + D_P\nabla^2\delta P_x, \tag{14}$$

using Fourier transformation,

$$\delta Y(\mathbf{k},S) = \int d\mathbf{r}\exp(i\mathbf{k}\cdot\mathbf{r})\exp(St)dt, \tag{15}$$

we get linear equation in Fourier space,

$$\partial_t \begin{pmatrix} \delta\rho \\ \delta P_z \\ \delta P_x \end{pmatrix} = \mathcal{M}\begin{pmatrix} \delta\rho \\ \delta P_z \\ \delta P_x \end{pmatrix},$$

where matrix $\mathcal{M}$ is given by coefficient of different terms in Eqs. (12), (13), and (14). We can solve above coupled equation for mode S. If the real part of S, $\mathrm{Re}[S] > 0$ homogeneous polarized state is unstable and if $\mathrm{Re}[S] < 0$, homogeneous polarized state is stable to small perturbation. We can solve for modes analytically for two different directions $\theta = 0$ and $\frac{\pi}{2}$, where θ is the angle between wave vector $\mathbf{q}$ and ordering direction. For $\theta = \frac{\pi}{2}$, S is determined by

$$(S + vP_0iq + D_\rho q^2)(S + D_P q^2) - \frac{v^2}{2}q^2 = 0, \tag{16}$$

and both modes are always stable. For $\theta = 0$,

$$(S + vP_0iq + D_\rho q^2)(S + 2\alpha_1(\eta) + D_P q^2) + \frac{v^2}{2}q^2 = 0. \tag{17}$$

Hence,

$$\mathrm{Re}[2S] = -\alpha_1(\eta) - \bar{D}q^2 \pm \frac{\frac{1}{2}v^2q^2\left(\frac{3}{8}\rho_0^2 + 1\right)}{2\alpha_1(\eta) + \bar{D}q^2}, \tag{18}$$

where $\bar{D} = D_\rho + D_P$, one of the modes can become unstable if

$$\tfrac{1}{2}v^2q^2\left(\tfrac{3}{8}\rho_0^2 + 1\right) > (\alpha_1(\eta) + \bar{D}q^2)(2\alpha_1(\eta) + \bar{D}q^2), \tag{19}$$

as we approach the critical point from the subcritical regime. Very close to critical point, we can write $\eta = \eta_c + \eta - \eta_c = \eta_c + \Delta\eta$, where η_c is the critical value of η at which $\alpha_1(\eta)$ changes sign and $\Delta\eta = \eta - \eta_c$, and since we are approaching critical point from below $\Delta\eta < 0$. Close to critical point we can expand $\alpha_1(\eta)$ about the critical η_c,

$$\begin{aligned}\alpha_1(\eta) &= \alpha_1(\eta_c) + \alpha_1'(\eta_c)\Delta\eta + \mathcal{O}(\Delta\eta)^2 \\ &= \alpha_1(\eta_c) - \alpha_1'(\eta_c)|\Delta\eta| + \mathcal{O}(\Delta\eta)^2,\end{aligned} \tag{20}$$

where $\alpha_1'(\eta_c) = \frac{\partial\alpha_1}{\partial\eta}|_{\eta_c}$. Since $\alpha_1(\eta) = \eta_c^2(1 - \frac{\eta^2}{\eta_c^2})$, hence $\alpha_1'(\eta_c) = -2\eta_c$, and we can write, up to linear order in $\Delta\eta$ as $\eta \to \eta_c$,

$$\begin{aligned}\alpha_1(\eta) &= \alpha_1(\eta_c) + 2\eta_c|\Delta\eta| + \mathcal{O}(\Delta\eta)^2 \\ &= |\Delta\eta|\big((\eta_c + \eta) + 2\eta_c\big) + \mathcal{O}(\Delta\eta)^2 \\ &= 4|\Delta\eta|\eta_c + \mathcal{O}(\Delta\eta)^2.\end{aligned} \tag{21}$$

However, the state is unstable if $\mathrm{Re}[S] > 0$ and stable if $\mathrm{Re}[S] < 0$. Hence, the condition for instability to leading order in $\Delta\eta$ and for small q limit is

$$v^2\left(\tfrac{3}{8}\rho_0^2 + 1\right) > 24|\Delta\eta|\eta_c\bar{D}. \tag{22}$$

As we approach critical point, instability is more pronounced and the smaller the value of η_c, instability occurs at a small v value. As shown in Fig. 11 and Eq. (11), η_c decreases as we decrease n. Hence, for small n instability appears at smaller v as shown in Fig. 12. We can also estimate critical wave vector at the onset of instability close to the critical point:

$$\bar{D}^2q_c^2 = \tfrac{1}{2}v^2\left(\tfrac{3}{8}\rho_0^2 + 1\right) - 12\eta_c|\Delta\eta|\bar{D}. \tag{23}$$

Hence, in the subcritical regime, as we approach closer and closer to the critical point, $\alpha_1(\eta)$ is small and instability will occur at a larger wave vector or a smaller length. Also, instability occurs at large q_c for small η_c (Fig. 13), and this is in agreement with our numerical simulation where we find

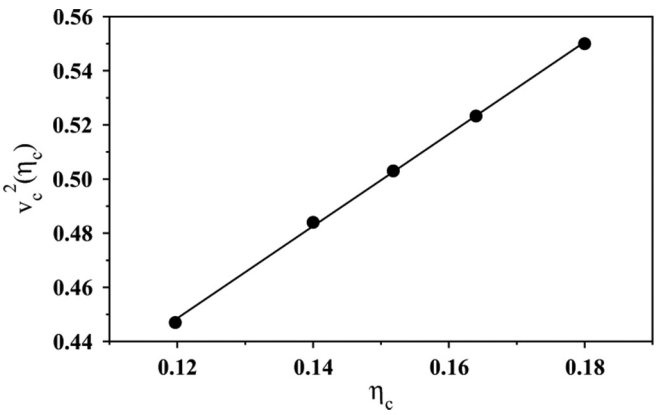

FIG. 12. Plot of critical v_c^2 vs. η_c for various n values. The value of η_c is estimated from numerical simulation for corresponding n value and the critical v_c is calculated from Eq. (22) for fixed density $\rho_0 = 0.125$.

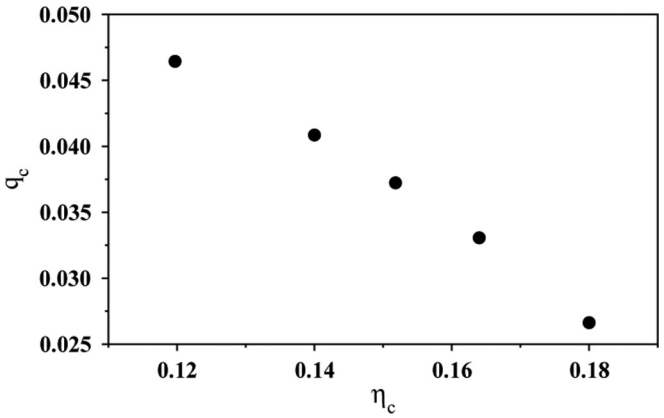

FIG. 13. Plot of critical wave vector q_c vs. η_c below which instability occur Eq. (23) for speed $v = 0.5$ and density $\rho_0 = 0.125$. Critical wave vector decreases with decreasing η_c and hence decreasing n.

formation of bands occurring at larger system size L as we go from the first ($n = 1$) neighbor to the second ($n = 2$) neighbor.

VI. SUMMARY

We have studied the collective behavior of a binary flock using Vicsek dynamics. In this flock the velocity of an agent depends on the velocities of its nth topological neighbor and its own. The velocity field of all agents are updated synchronously maintaining the periodic boundary condition on a collection of agents confined within a two-dimensional square space. Extensive numerical simulations reveal that for all values of n, a order to disorder phase transition takes place at certain critical threshold η_c of the noise parameter. In particular, for $n = 1$, it is a different kind of discontinuous transition: The long time stationary state of the system is either in the ordered phase, or in the disordered phase. At a certain η_c for $n = 1$ it switches over from one phase to the other. The case of $n = 2$ exhibits ordinary discontinuous transition where, around the critical point, the system flip flops between the two metastable states corresponding to the ordered and disordered phases. Probability distribution of the order parameter has been observed to be characterized by doubly humped function, whereas the fourth order Binder cumulant exhibits a negative dip at the critical noise strength. For $n \geqslant 3$ the system exhibits continuous transitions, signatures of which are evident in the continuous variation of their order parameters against noise strengths, continuous variation of their Binder cumulants and singly peaked distributions of their order parameters.

Persistence time is the duration of the time interval through which an agent has a specific topological neighbor. The probability distribution of persistence times has been found to follow nice power law decaying functions and independent of the value of the topological neighbor n. Further, we have studied the information spreading dynamics in the binary flocks. How long it takes on the average to spread an information localized at a certain agent to spread to all agents of the system? It has been seen that the mean value of this time decays like a power law as the noise level increases from zero.

Finally, this system of binary flocks has been studied again using the hydrodynamic equations of motion. Linear stability analysis of the homogeneous polarized state close to the order-disorder transition has been done. The average correlation between a pair of agents, who are the topological neighbors, has been calculated. Using the value of this quantity, the critical noise strength has been estimated and the correspondence has been found to be good.

ACKNOWLEDGMENTS

Useful advice from T. Vicsek is thankfully acknowledged. S.M. acknowledges financial support (under Inspire faculty award) from the Department of Science and Technology, India.

[1] T. Vicsek and A. Zafeiris, Phys. Rep. **517**, 71 (2012).
[2] J. Toner, Y. Tu, and S. Ramaswamy, Ann. Phys. **318**, 170 (2005).
[3] J. Toner and Y. Tu, Phys. Rev. Lett. **75**, 4326 (1995); Phys. Rev. E **58**, 4828 (1998).
[4] D. L. Blair and A. Kudrolli, Phys. Rev. E **67**, 041301 (2003).
[5] V. Narayan, N. Menon, and S. Ramaswamy, J. Stat. Mech. (2006) P01005; V. Narayanan, S. Ramaswamy, and N. Menon, Science **317**, 105 (2007).
[6] M. C. Marchetti, J. F. Joanny, S. Ramaswamy, T. B. Liverpool, J. Prost, Madan Rao, and R. Aditi Simha, Rev. Mod. Phys. **85**, 1143 (2013).
[7] A. Czirok, H. E. Stanley, and T. Vicsek, J. Phys. A **30**, 1375 (1997); P. Szabó, M. Nagy and T. Vicsek, Phys. Rev. E **79**, 021908 (2009).
[8] T. Vicsek, A. Czirók, E. Ben-Jacob, I. Cohen, and O. Shochet, Phys. Rev. Lett. **75**, 1226 (1995).
[9] B. Bhattacherjee, K. Bhattacharya, and S. S. Manna, Frontiers Phys. **1**, 1 (2014).
[10] M. Ballerini, N. Cabibbo, R. Candelier, A. Cavagna, E. Cisbani, I. Giardina, V. Lecomte, A. Orlandi, G. Parisi, A. Procaccini, M. Viale, and V. Zdravkovic, Proc. Natl. Acad. Sci. U.S.A. **105**, 1232 (2008).
[11] M. Aldana, V. Dossetti, C. Huepe, V. M. Kenkre, and H. Larralde, Phys. Rev. Lett. **98**, 095702 (2007).
[12] M. Aldana and C. Huepe, J. Stat. Phys. **112**, 135 (2003); C. Huepe and M. Aldana, Physica A **387**, 2809 (2008).
[13] H. Chaté, F. Ginelli, Guillaume Grégoire, and F. Raynaud, Phys. Rev. E **77**, 046113 (2008).
[14] H. Chaté, F. Ginelli, and R. Montagne, Phys. Rev. Lett. **96**, 180602 (2006); H. Chaté, F. Ginelli, and G. Grégoire, *ibid.* **99**, 229601 (2007).
[15] F. Ginelli and H. Chaté, Phys. Rev. Lett **105**, 168103 (2010).
[16] A. Peshkov, S. Ngo, E. Bertin, H. Chaté, and F. Ginelli, Phys. Rev. Lett. **109**, 098101 (2012).
[17] T. Feder, Phys. Today **60**, 28 (2007).
[18] G. Grégoire and H. Chaté, Phys. Rev. Lett. **92**, 025702 (2004).
[19] M. Nagy, I. Daruka, and T. Vicsek, Physica A **373**, 445 (2007).
[20] K. Binder, K. Vollmayr, H.-P. Deutsch, J. Reger, M. Scheucher, and D. P. Landau, Int. J. Mod. Phys. C **03**, 1025 (1992).
[21] E. Bertin, M. Droz, and G. Grégoire, J. Phys A: Math. Theor. **42**, 445001 (2009).